Lecture 11

Ch. 11 Critically stressed faults and fluid flow (18, 20 May 2020)

Ki-Bok Min, PhD

Professor
Department of Energy Resources Engineering
Seoul National University

SEOUL NATIONAL UNIVERSITY

Disclaimer

SEOUL NATIONAL UNIVERSITY

- Materials in these slides cannot be used without the written consent from the instructor

Critically stressed faults and fluid flow
Importance

- Critically stressed faults and fluid flow
  - Fractures are often main conduits for fluid flow in low-permeable formations
- Importance of stress analysis in fault in relation to in situ stress
  - In situ stress constraints
  - Fluid flow analysis – oil and gas
  - Hydraulic stimulation – shear stimulation for shale gas and geothermal
  - Earthquake analysis
- Topics
  - Influence of fracture and faults on reservoir permeability
  - Geomechanical control on fault sealing and leakage in fault bounded reservoir
  - Dynamic constraints on hydrocarbon column heights and reservoir pressure in fault bounded reservoir
    - We may go beyond the interpretations based on structural closure

Chapter 4. Rock Failure in compression, tension and shear

- In situ stress constraints

Limits on in situ stress from the frictional strength of faults

- Normal and shear stress at fractures

$$\tau_f = 0.5(\sigma_1 - \sigma_3)\sin 2\beta$$
$$\sigma_n = 0.5(\sigma_1 + \sigma_3) + 0.5(\sigma_1 - \sigma_3)\cos 2\beta$$

- Optimally oriented fracture

$\beta = 45° + 1/2\tan^{-1}\mu$

- $\mu = 1$, $\beta = 67.5°$
- $\mu = 0.6$, $\beta \sim 60°$
- $\mu \sim 0$, $\beta \sim 45°$

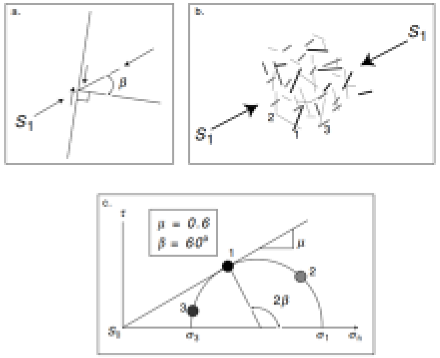

Figure 4.27. (a) Frictional sliding on an optimally oriented fault in two dimensions. (b) One can consider the Earth's crust as containing many faults at various orientations, only some of which are optimally oriented for frictional sliding. (c) Mohr diagram corresponding to faults of different orientations. The faults shown by black lines in (b) are optimally oriented for failure (labeled 1 in b and c), those shown in light gray in (b) (and labeled 2 in b and c) in (b) trend more perpendicular to S_{Hmax} and have appreciable normal stress and little shear stress. The faults shown by heavy gray lines and labeled 3 in (b) are more parallel to S_{Hmax} have significantly less shear stress and less normal stress than optimally oriented faults as shown in (c).

The critically stressed crust

- EQ triggered by small stress change
  - Experiment at KTB borehole in Germany

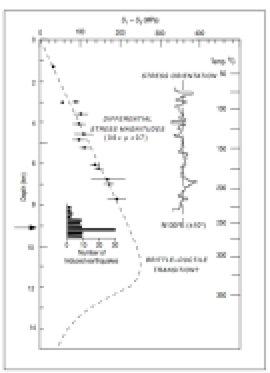

Figure 4.26. Stress measurements in the KTB scientific research well indicate a strong crust, in a state of failure equilibrium as predicted by Coulomb theory and laboratory-derived coefficients of friction of 0.6–0.7 (after Zoback and Harjes 1997). The arrow at 9.2 km depth indicates where the fluid injection experiment occurred.

- In situ stress measurement
  - Byerlee's law seems to work
  - Earth crust appears to be in a state of (failure) equilibrium

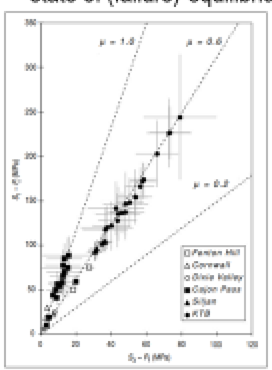

Figure 4.28. In situ stress measurements in relatively deep wells in crystalline rock indicate that stress magnitudes seem to be controlled by the frictional strength of faults with coefficients of friction between 0.6 and 1.0. After Zoback and Townend (2001). *Reprinted with permission of Elsevier.*

Stress polygon

- Diagram showing the range of possible stress state at a given depth and pore pore pressure
  - Stress state above a $S_{Hmax} = S_{hmin}$

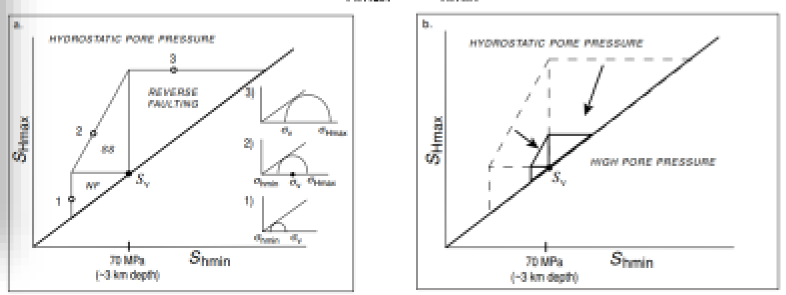

Normal faulting $\frac{\sigma_1}{\sigma_3} = \frac{S_v - P_p}{S_{hmin} - P_p} \le [(\mu^2+1)^{1/2} + \mu]^2$

Strik-slip faulting $\frac{\sigma_1}{\sigma_3} = \frac{S_{Hmax} - P_p}{S_{hmin} - P_p} \le [(\mu^2+1)^{1/2} + \mu]^2$

Reverse faulting $\frac{\sigma_1}{\sigma_3} = \frac{S_{Hmax} - P_p}{S_v - P_p} \le [(\mu^2+1)^{1/2} + \mu]^2$

Fractured reservoirs and fluid flow
Critically stressed fault – Stress polygon

- Hypothesis of 'critically stressed fault' can be applied to constrain the range of in situ stress
  - Stress polygon help to draw the range of in situ stress
  - Stress state above the line of $S_{Hmax} = S_{hmin}$

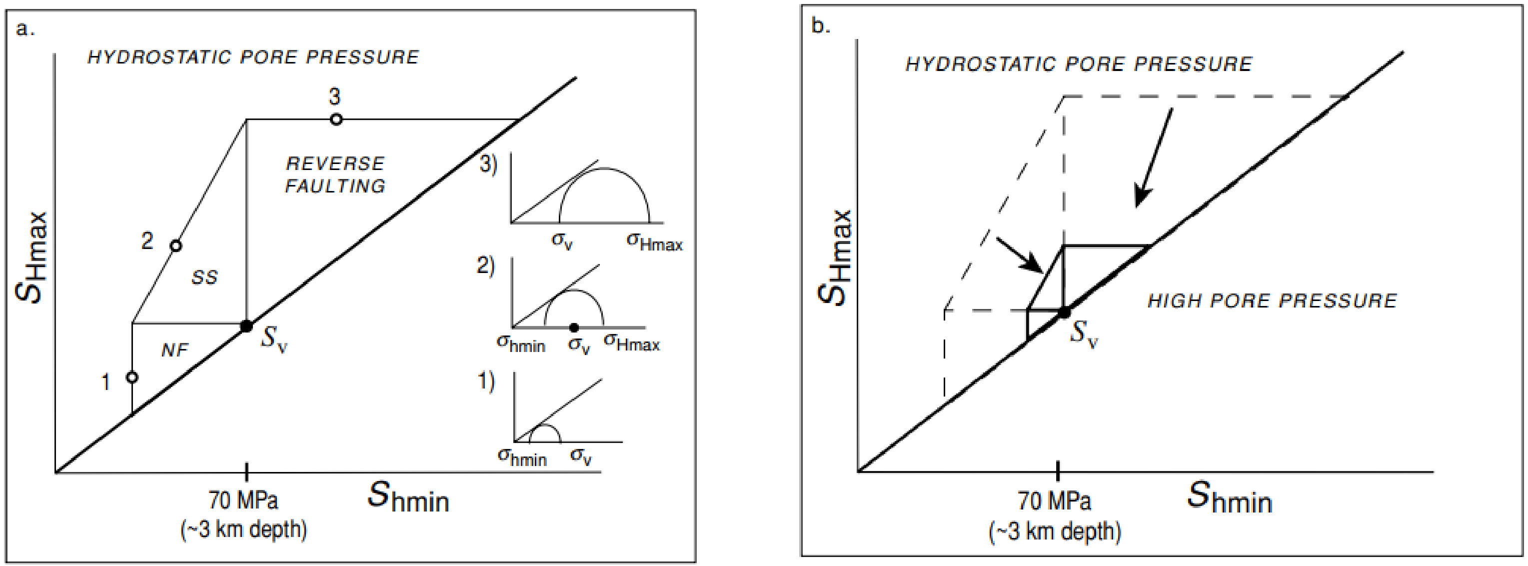

Normal faulting $\frac{\sigma_1}{\sigma_3} = \frac{S_v - P_p}{S_{hmin} - P_p} \le [(\mu^2+1)^{1/2} + \mu]^2$

Strik-slip faulting $\frac{\sigma_1}{\sigma_3} = \frac{S_{Hmax} - P_p}{S_{hmin} - P_p} \le [(\mu^2+1)^{1/2} + \mu]^2$

Reverse faulting $\frac{\sigma_1}{\sigma_3} = \frac{S_{Hmax} - P_p}{S_v - P_p} \le [(\mu^2+1)^{1/2} + \mu]^2$

Zoback MD, 2007, Reservoir Geomechanics, Cambridge University Press

Fractured reservoirs and fluid flow
Critically stressed fault – observations

- In situ stress measurement
  - Byerlee's law seems to work
  - Earth crust appears to be in a state of (failure) equilibrium

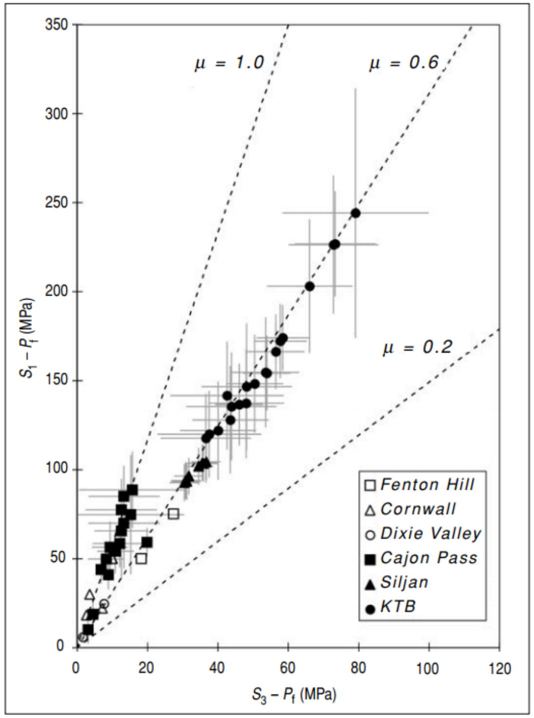

Figure 4.26. *In situ* stress measurements in relatively deep wells in crystalline rock indicate that stress magnitudes seem to be controlled by the frictional strength of faults with coefficients of friction between 0.6 and 1.0. After Zoback and Townend (2001). *Reprinted with permission of Elsevier.*

Zoback MD, 2007, Reservoir Geomechanics, Cambridge University Press

Fractured reservoirs and fluid flow
Critically stressed fault

- Identifying active faults is important both hydraulically & mechanically
- *"faults that are mechanically alive are hydraulically alive and faults that are mechanically dead are hydraulically dead"*

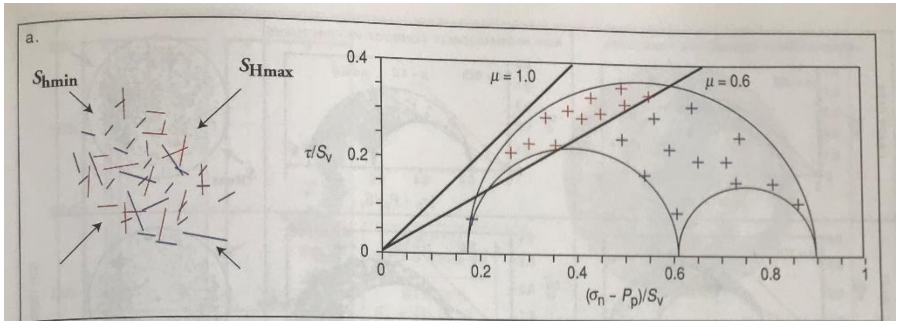

Fractures with varying orientations are under various combinations of normal stress + shear stress

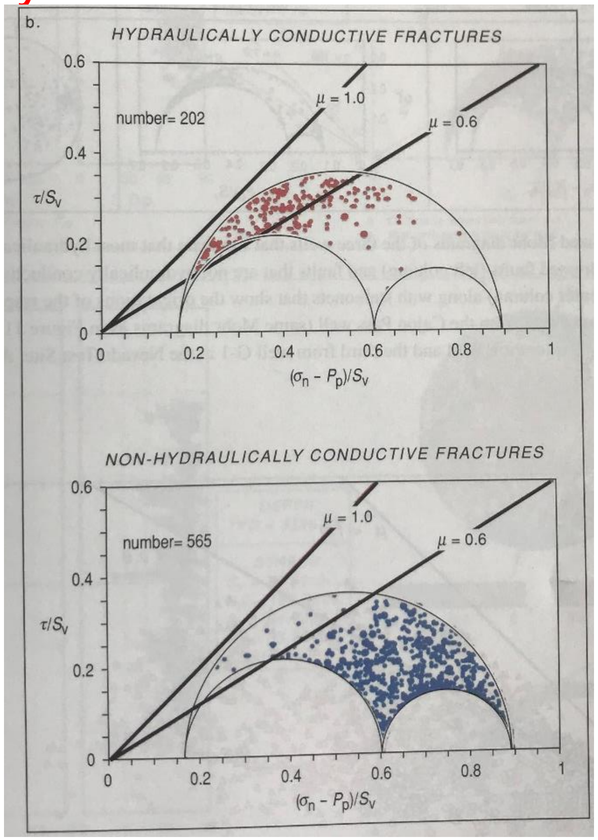

Permeable faults and impermeable faults plotted with respect to failure criterion and stress condition (Cajon Pass scientific borehole near the San Andreas fault)

Zoback MD, 2007, Reservoir Geomechanics, Cambridge University Press

Fractured reservoirs and fluid flow
Critically stressed fault – basic law

- Shear failure of a fault (fracture) – Coulomb Failure criterion

$$\frac{\tau}{\sigma_n} = \mu$$

***μ*: Coefficient of friction**

$\sigma_n = S_n - P_p$

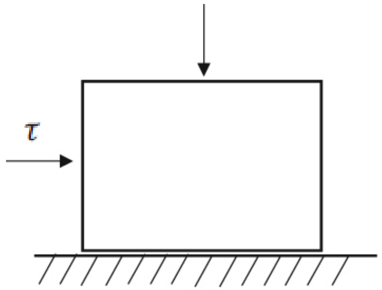

- Coulomb Failure Function (CFF)
  - Shear stress minus resistance. (-) no slip, (+) slip

$$\mathrm{CFF} = \tau - \mu\sigma_n$$

$CFF = \tau - \mu(S_n - P_p)$

- Critical pore pressure

$$P_p^{crit} = S_n - \tau/\mu$$

Fractured reservoirs and fluid flow
Critically stressed fault – basic law

SEOUL NATIONAL UNIVERSITY

- Range of μ (Byerlee's law)
  - At higher effective stress (10 MPa)

$$0.6 \leq \mu \leq 1.0$$

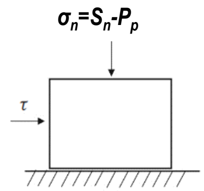

  - Coefficient of friction in general lie in those ranges regardless of rock type and roughness
  - John Jaeger
    "There are only two things you need to know about friction. It is always 0.6 and it will always make a monkey out of you."
  - Shaly rock μ < *0.6*

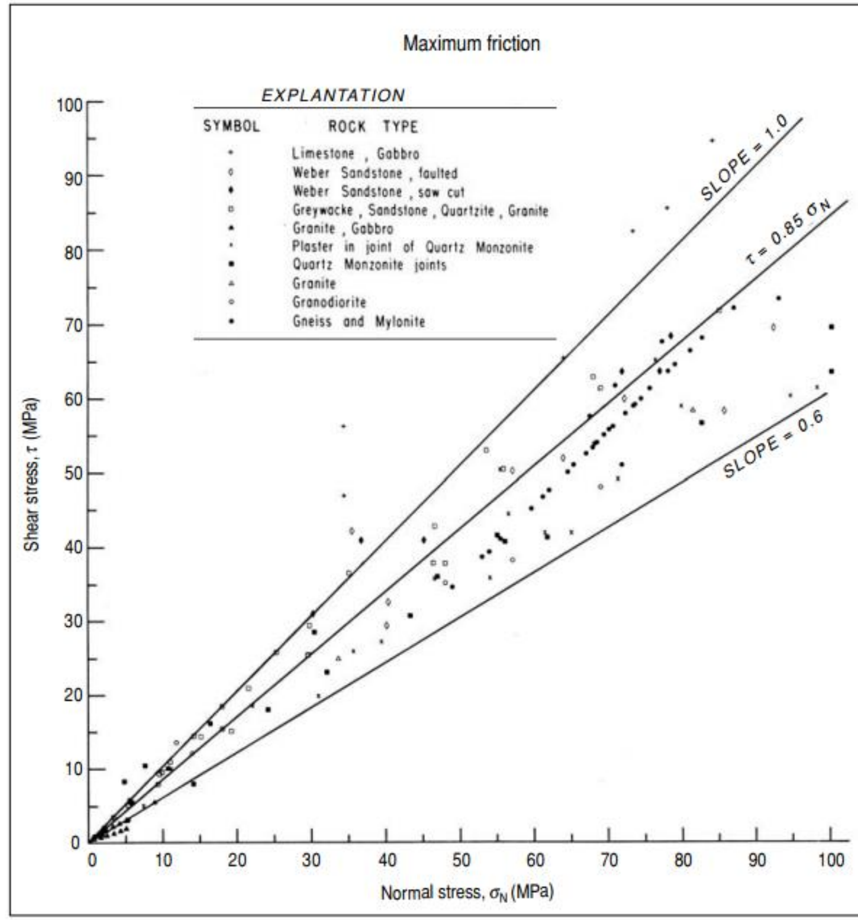

Figure 4.23. Rock mechanics tests on wide range of rocks (and plaster in a rock joint) demonstrating that the coefficient of friction (the ratio of shear to effective normal stress) ranges between 0.6 and 1.0 at effective confining pressures of interest here. Modified after Byerlee (1978).

Zoback MD, 2007, Reservoir Geomechanics, Cambridge University Press

Fractured reservoirs and fluid flow
Critically stressed fault – mechanical behavior

SEOUL NATIONAL UNIVERSITY

- Normal mechanical behavior
  - Unit: Stress/length (MPa/m)
  - Linear model $\sigma_n = K_n \delta_n$
  - Non-linear model

$$\delta_n = \frac{\sigma_n}{c + d\sigma_n}$$

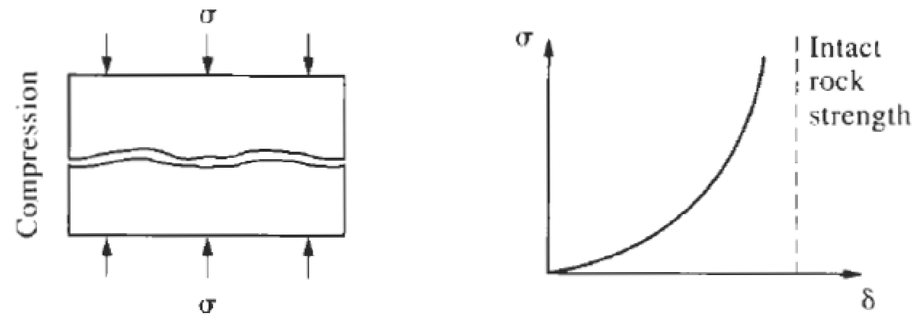

- Shear mechanical behavior
  - Unit: Stress/length (MPa/m)
  - Linear model $\sigma_s = K_s \delta_s$
  - Non-linear model: e.g., Barton's equation
  - Dilation angle $\phi_{dilation} = \tan^{-1}\left(\dfrac{\text{normal dilation}}{\text{shear displacement}}\right)$

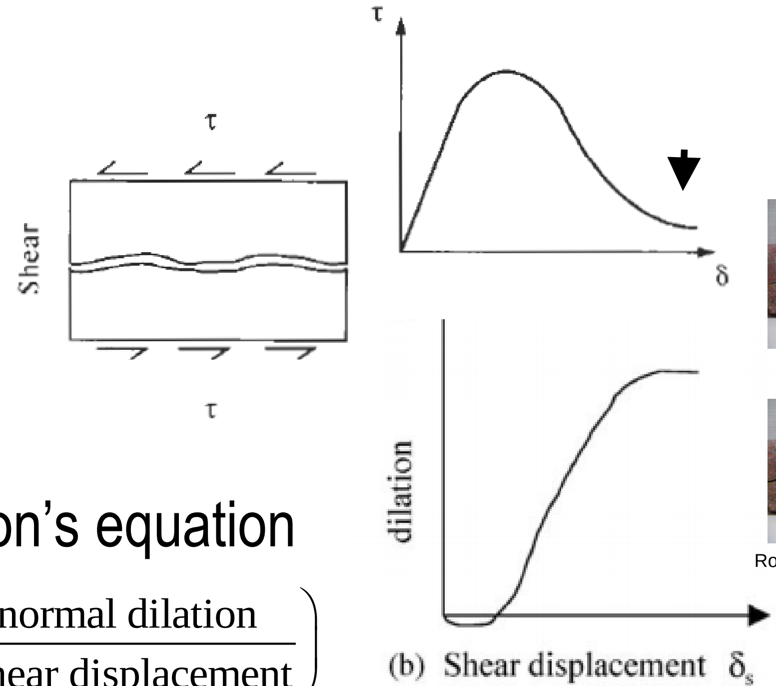

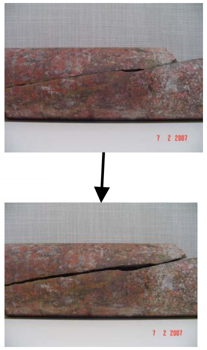

Rothert & Baisch (2010)

Rothert E & Baisch S, 2010, Passive Seismic Monitoring: Mapping Enhanced Fracture Permeability, 10th World Geothermal Congress, Paper No.3161

Fractured reservoirs and fluid flow
Critically stressed fault – fluid flow along a fracture/fault

SEOUL NATIONAL UNIVERSITY

Real rock fracture

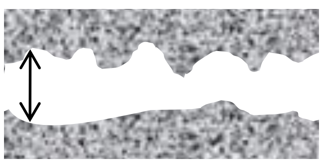

Idealization

Conceptual model

Idealized rock fracture

Aperture (e, or b): size of opening measured normal to the fracture wall

$$v = -\frac{1}{8\mu}\left(e^2 - 4y^2\right)\frac{d(\rho_w gh)}{dx}$$

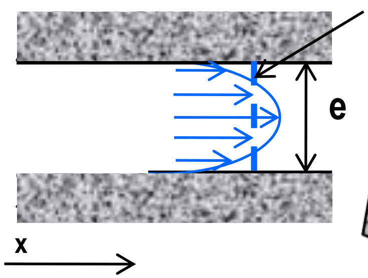

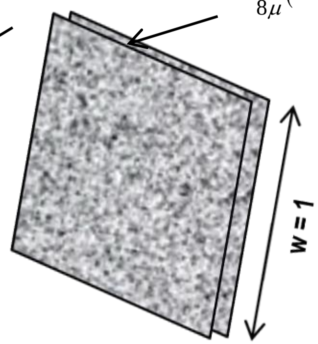

$$Q = \int_{-\frac{e}{2}}^{\frac{e}{2}} v(wdy) = -\frac{we^3}{12\mu}\frac{d}{dx}(\rho_w gh)$$

$$Q = -\frac{e^3}{12\mu}\frac{d}{dx}(\rho_w gh) = -\frac{\rho_w ge^3}{12\mu}\frac{dh}{dx}$$

$$K = \frac{\rho gk}{\mu}$$

$\rho ge^2/12\mu$ = hydraulic conductivity (K) of a fracture
$\rho ge^3/12\mu$ = transmissivity (T) of a fracture
$e^2/12$ = permeability (k) of a fracture

$$Q = -\frac{\rho_w ge^3}{12\mu}\frac{\partial h}{\partial x}$$

$$Q = -\frac{e^3}{12\mu}\frac{\partial p}{\partial x} \leftarrow$$

with zero elevation

ρ_w: density of fluid
g: acceleration of gravity
μ: viscosity (=η)

– Cubic law: for a given gradient in pressure and unit width (w), flow rate through a fracture is proportional to the **cube** of the fracture aperture.

plate approximation for fluid flow through a planar fracture. For a given fluid viscosity, η, the volumetric flow rate, Q, resulting from a pressure gradient, ∇P, is dependent on the cube of the separation between the plates, b,

$$Q = \frac{b^3}{12\eta}\nabla P \qquad (5.1)$$

Critically stressed fault – shear dilation

- Shear dilation observation (Olsson & Barton, 2001)

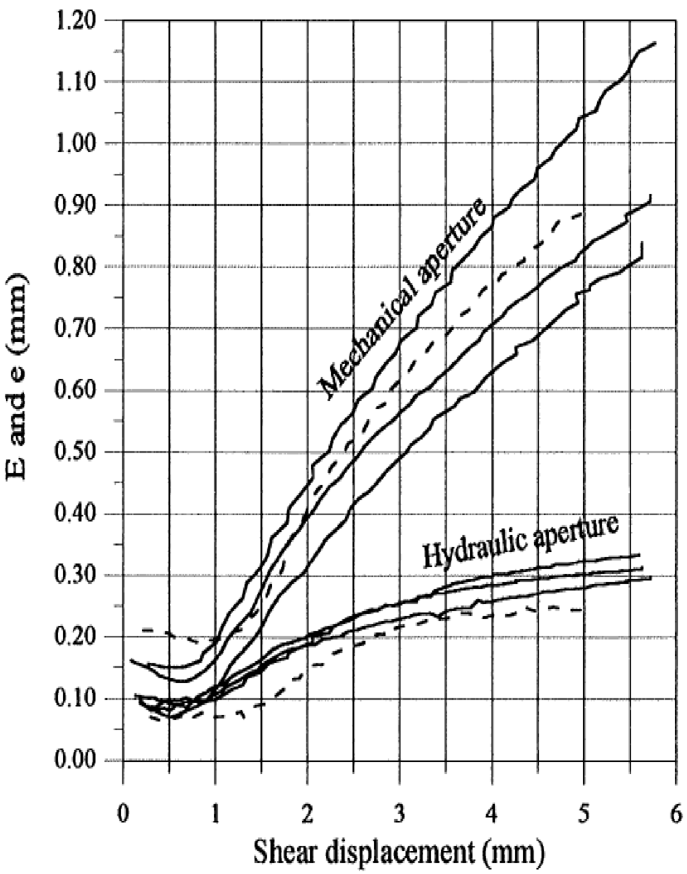

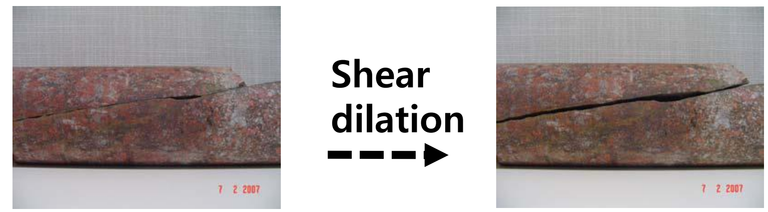

Rothert & Baisch (2010)

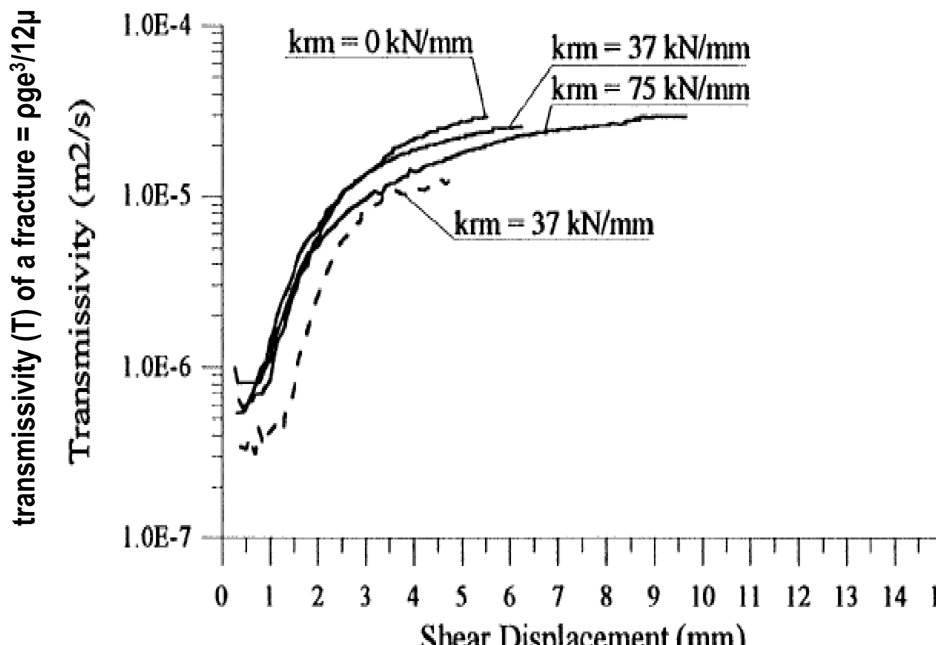

Olsson, R. and N. Barton (2001). "An improved model for hydromechanical coupling during shearing of rock joints." International Journal of Rock Mechanics and Mining Sciences 38(3): 317-329.

Rothert E & Baisch S, 2010, Passive Seismic Monitoring: Mapping Enhanced Fracture Permeability, 10th World Geothermal Congress, Paper No.3161

Fractured reservoirs and fluid flow
Critically stressed fault – shear dilation

SEOUL NATIONAL UNIVERSITY

- Brecciation through shearing

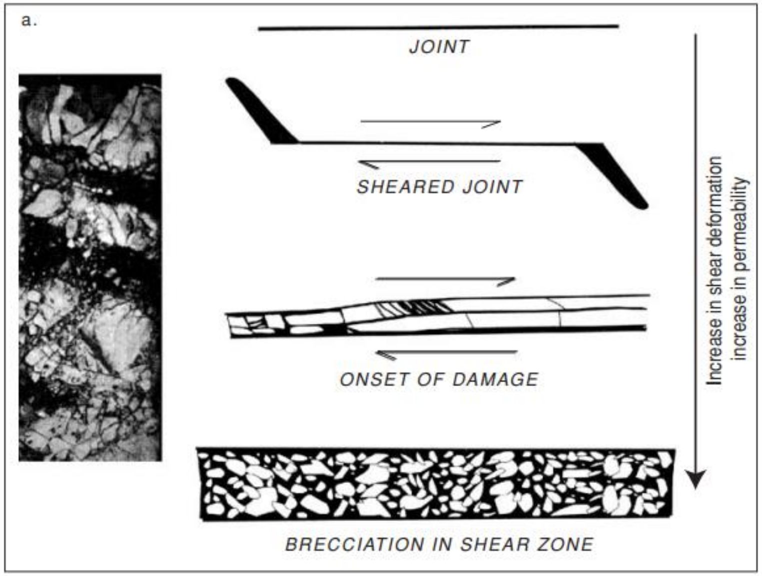

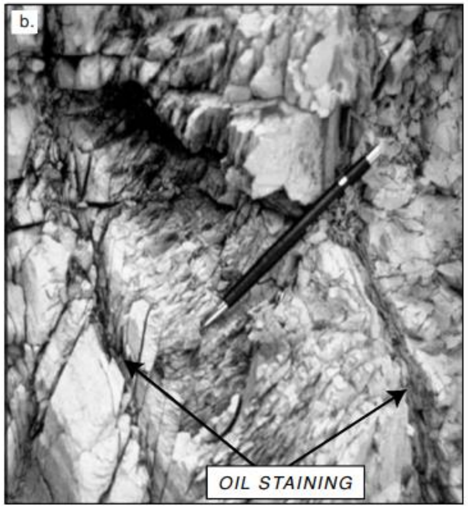

Figure 5.2. Schematic illustration of the evolution of a fault from a joint (after Dholakia, Aydin *et al*. 1998). As shear deformation occurs, brecciation results in interconnected porosity thus enhancing formation permeability. In the Monterey formation of California, oil migration is strongly influenced by the porosity generated by brecciation accompanying shear deformation on faults. This can be observed at various scales in core (a) and outcrop (b). *AAPG© 1998 reprinted by permission of the AAPG whose permission is required for futher use.*

Zoback MD, 2007, Reservoir Geomechanics, Cambridge University Press

Fractured reservoirs and fluid flow

Critically stressed fault – shear dilation and dilation angle

- Direct shear test on 57 single fractures (Glamheden, 2007)

	0.5 MPa	5 MPa	20 MPa
σ_n =	0.5 MPa	5 MPa	20 MPa
Ψ_{mean} =	14.6°	7.7°	3.2°

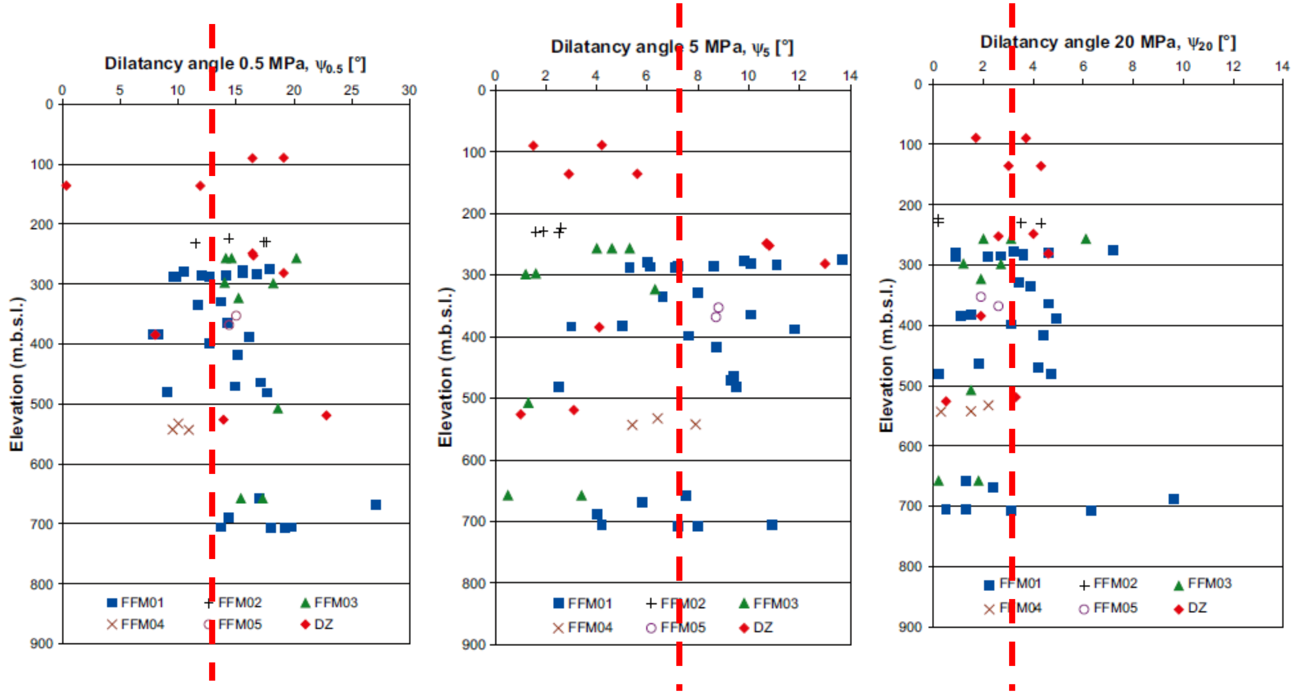

- Shear dilation varies a lot at moderate normal stress (~ 20 MPa, ~ 500 m)
- At deep depth, dilation seems fairly small but it still enhance permeability a great deal

Glamheden R, Fredriksson A, Röshoff K, Karlsson J, Hakami H and Christiansson R (2007), Rock Mechanics Forsmark. Site descriptive modelling Forsmark stage 2.2. SKB.

Critically stressed fault – shear dilation and dilation angle

- Example:
  - Stress dependent permeability of fractured rock (Min et al., 2004)

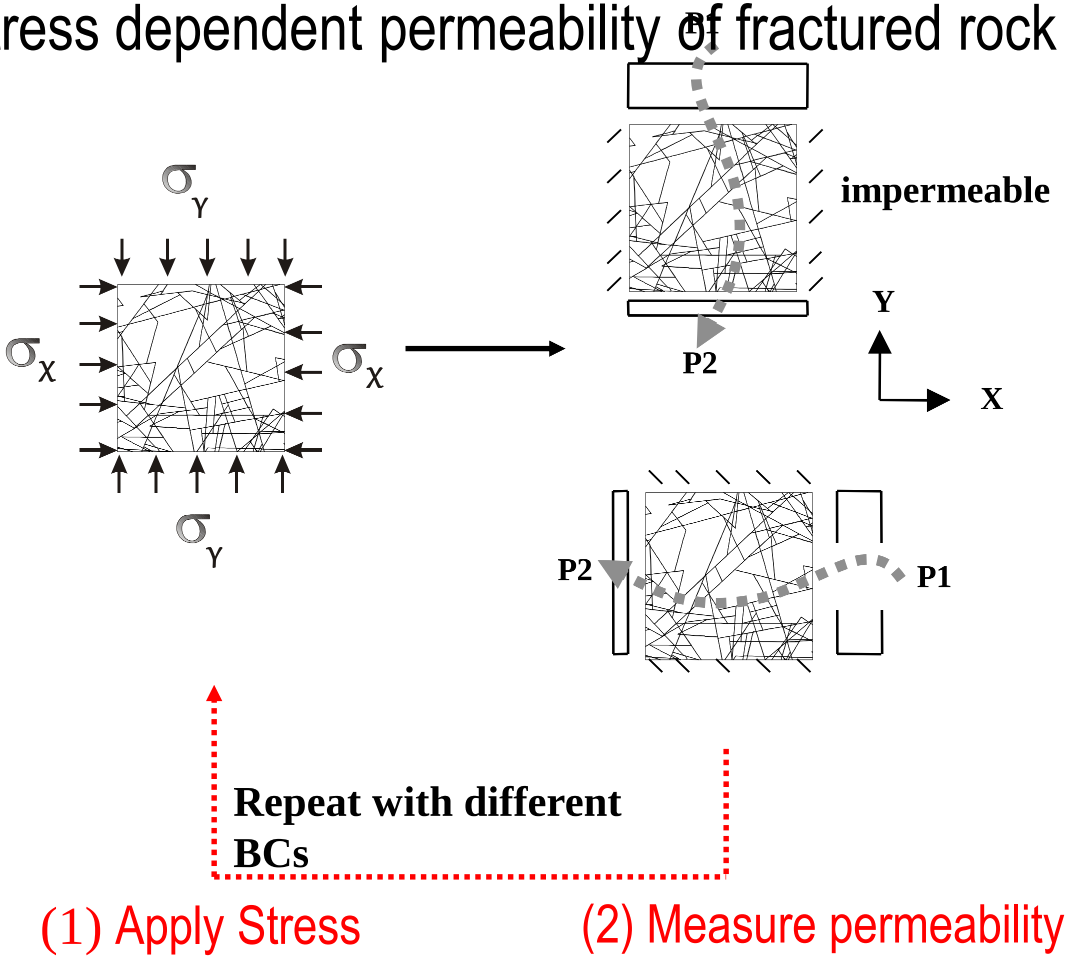

Min, KB, Rutqvist J, Tsang CF, Jing L (2004). "Stress-dependent permeability of fractured rock masses: a numerical study." International Journal of Rock Mechanics and Mining Sciences 41(7): 1191-1210.

Flowrates:

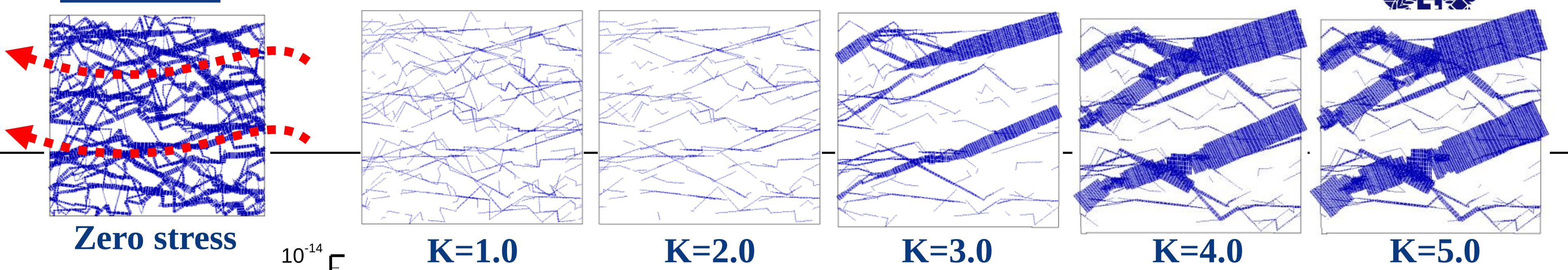

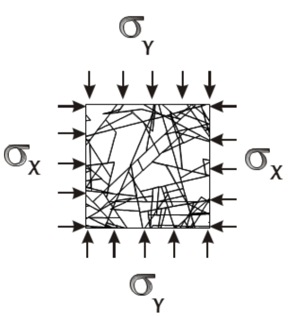

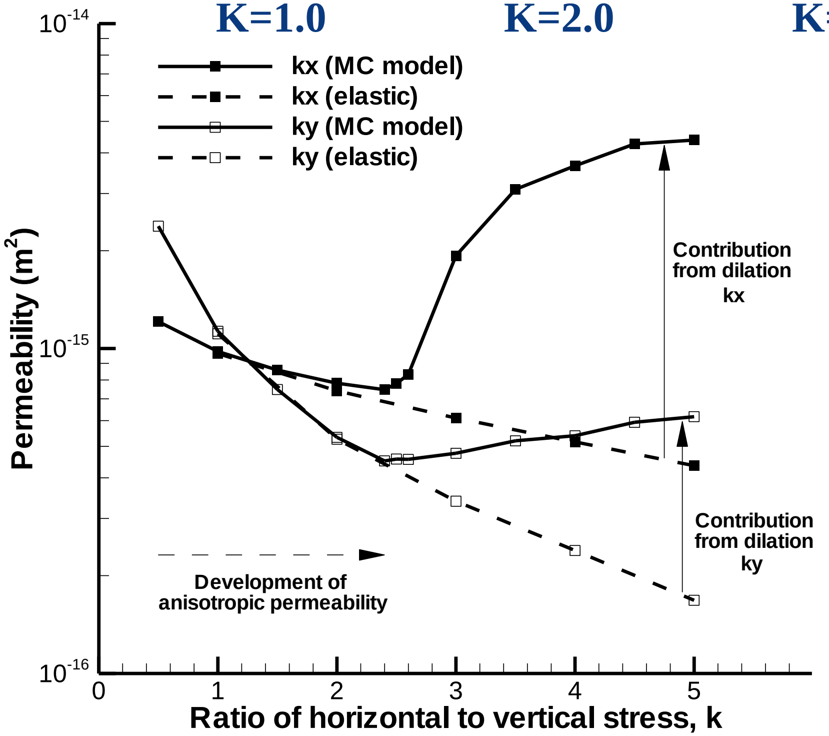

- Fluid flow enhancement by critically stressed fault/fracture
- Critically stress fault/fracture carry most of fluid
- This partly explains why fluid flow in a few fractures are dominating the fluid behaviour

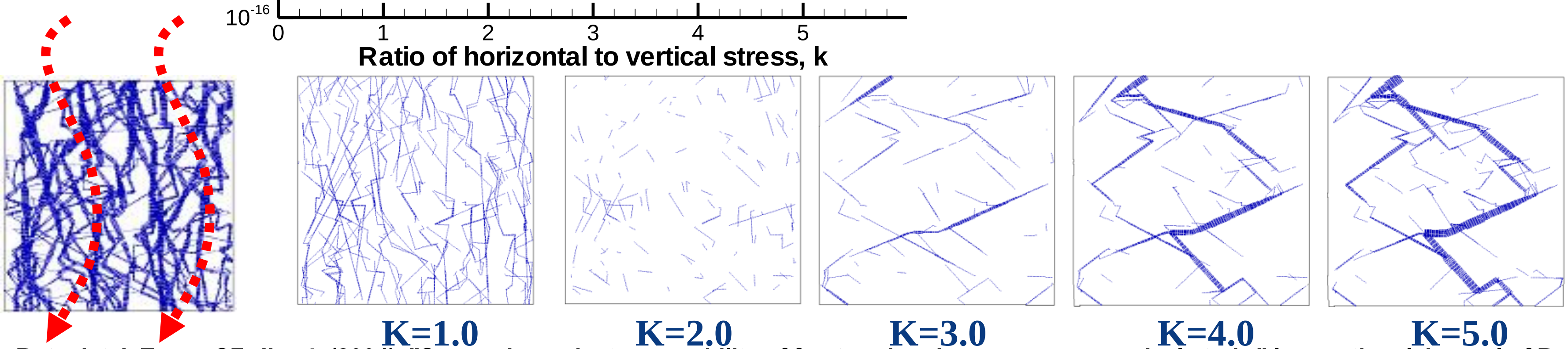

Min, KB, Rutqvist J, Tsang CF, Jing L (2004). "Stress-dependent permeability of fractured rock masses: a numerical study." International Journal of Rock Mechanics and Mining Sciences 41(7): 1191-1210.

Critically stressed fault – shear dilation and anisotropic fluid flow

- Shearing induce anisotropic flow in a fracture plane:
  - Flow perpendicular to the shearing direction is much larger than that in parallel to the shearing

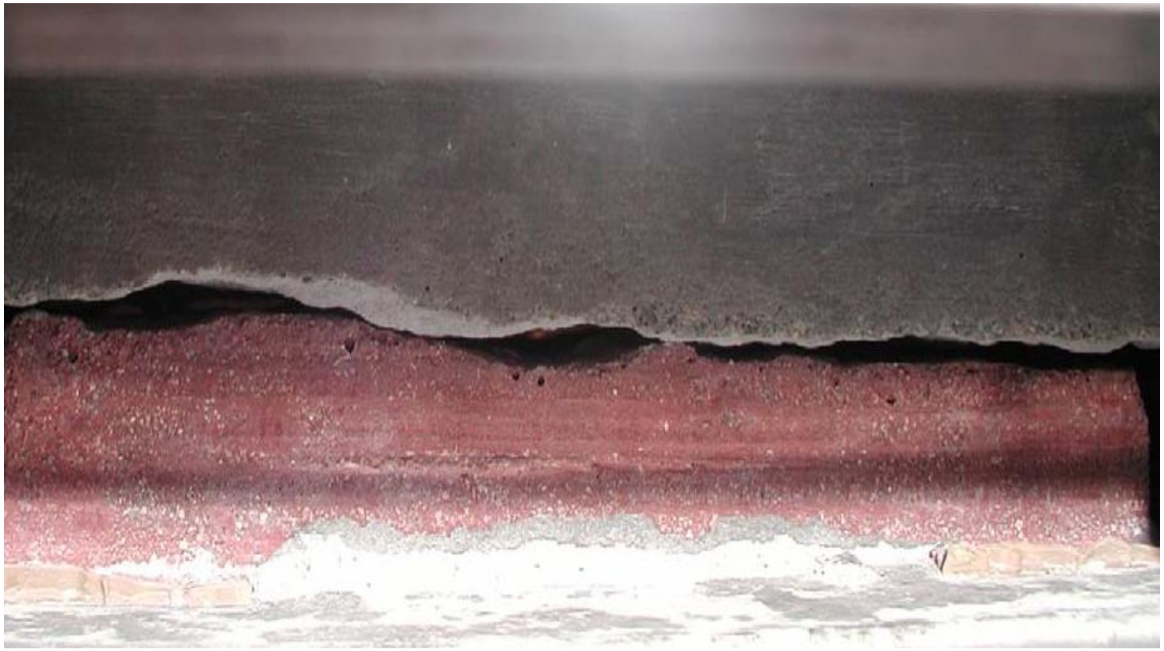

Rock fracture replica after shearing

Koyama, T., et al. (2006). "Numerical simulation of shear-induced flow anisotropy and scale-dependent aperture and transmissivity evolution of rock fracture replicas, IJRMMS;43(1): 89-106.

Fractured reservoirs and fluid flow
Calculation of normal and shear stress on a fault

SEOUL NATIONAL UNIVERSITY

- Calculation of normal and shear stress on the fault with given orientation
  - Input: in situ stress, fault orientation, friction coefficient
  - Normal (S_n) and shear (τ) stress acting on the plane
  - Analysis: Coulomb failure analysis

$$\mathrm{t} = \boldsymbol{S}\hat{n}$$

$$S_n = \hat{n} \cdot \mathrm{t}$$

$$\tau^2 = t^2 - S_n^2$$

$$\boldsymbol{S} = \begin{bmatrix} S_1 & 0 & 0 \\ 0 & S_2 & 0 \\ 0 & 0 & S_3 \end{bmatrix} = \begin{bmatrix} S_{\mathrm{Hmax}} & 0 & 0 \\ 0 & S_v & 0 \\ 0 & 0 & S_{\mathrm{hmin}} \end{bmatrix}$$

Fault orientation: $\hat{n} = (n_1, n_2, n_3)$

← unit normal vector

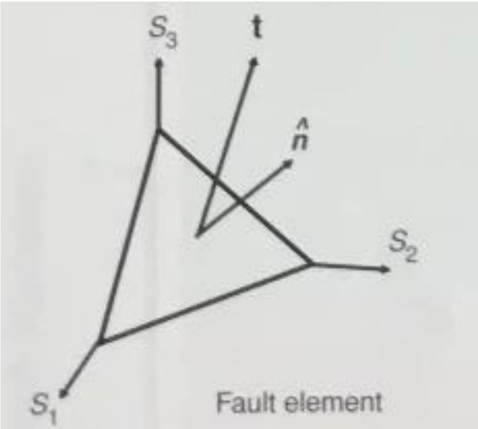

$$\tau = \mu(S_n - P_p)$$

Calculation of normal and shear stress on a fault

- Cauchy's formula
  - Input: stress tensor & unit normal vector of a plane (= fault)
  - Output: Traction vector (stress vector) at the plane (= fault)

☆ Cauchy's formula. stress + surface → vector at the surface.

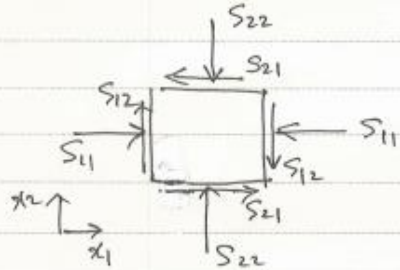

$$\begin{pmatrix} S_{11} & S_{12} \\ S_{21} & S_{22} \end{pmatrix}$$ stress in 2D.

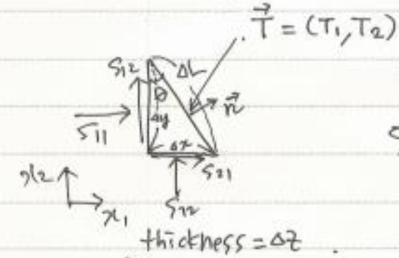

From Force Equilibrium,

$$\Sigma F_x = S_{11}\Delta y \Delta z + S_{21}\Delta x \Delta z - T_1 \Delta L \Delta z = 0$$

$$T_1 = S_{11}\frac{\Delta y}{\Delta L} + S_{21}\frac{\Delta x}{\Delta L}$$

$$\vec{n} = (n_x, n_y) = (\cos\theta, \sin\theta), \quad \frac{\Delta y}{\Delta L} = \cos\theta, \quad \frac{\Delta x}{\Delta L} = \sin\theta$$

$$T_1 = S_{11}\cos\theta + S_{21}\sin\theta = S_{11} n_x + S_{21} n_y.$$

$$\Sigma F_y = S_{22}\Delta x \Delta z + S_{12}\Delta y \Delta z - T_2 \Delta L \Delta z = 0.$$

$$T_2 = S_{12}\cdot\frac{\Delta y}{\Delta L} + S_{22}\frac{\Delta x}{\Delta L} = S_{12}\cos\theta + S_{22}\sin\theta$$
$$= S_{12} n_x + S_{22} n_y.$$

$$\vec{T} = \begin{pmatrix} T_1 \\ T_2 \end{pmatrix} = \begin{pmatrix} S_{11} & S_{21} \\ S_{12} & S_{22} \end{pmatrix}\begin{pmatrix} n_x \\ n_y \end{pmatrix} = \begin{pmatrix} S_{11} & S_{12} \\ S_{21} & S_{22} \end{pmatrix}\begin{pmatrix} n_x \\ n_y \end{pmatrix}.$$

In 3D,

$$\vec{T} = \begin{pmatrix} T_1 \\ T_2 \\ T_3 \end{pmatrix} = \begin{pmatrix} S_{11} & S_{12} & S_{13} \\ S_{21} & S_{22} & S_{23} \\ S_{31} & S_{32} & S_{33} \end{pmatrix}\begin{pmatrix} n_x \\ n_y \\ n_z \end{pmatrix} = [S]_{3\times3}[n]_{3\times1}$$

t in the Zoback (2007)

Knowing the stress S_{ij}, and a surface with unit outer normal vector $\vec{n}$ whose components are (n_x, n_y, n_z), we can calculate traction vector $\vec{T}$ (stress vector) acting on that surface. → Cauchy's formula

1. Calculation of normal and shear stress on a fault
   - Input: Traction vector (stress vector) and unit normal vector of a plane (fault)
   - Output: Normal and shear stress on the surface (fault)
2. Coefficient of friction
3. Pore pressure at the fault

- Calculation of Coulomb Failure function (CFF)

$$\mathrm{CFF} = \tau - \mu\sigma_n$$

$$CFF = \tau - \mu(S_n - P_p)$$

by choosing principal stresses aligned with axis x_1, x_2, x_3

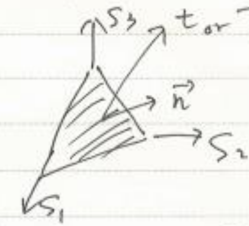

$$S_{ij} = [S] = \begin{pmatrix} S_1 & 0 & 0 \\ 0 & S_2 & 0 \\ 0 & 0 & S_3 \end{pmatrix}$$

t

$$T = \begin{pmatrix} T_1 \\ T_2 \\ T_3 \end{pmatrix} = \begin{pmatrix} S \end{pmatrix}\begin{pmatrix} n \end{pmatrix} = \begin{pmatrix} S_1 & 0 & 0 \\ 0 & S_2 & 0 \\ 0 & 0 & S_3 \end{pmatrix}\begin{pmatrix} n_1 \\ n_2 \\ n_3 \end{pmatrix} = \begin{pmatrix} S_1 n_1 \\ S_2 n_2 \\ S_3 n_3 \end{pmatrix}$$

(normal stress)

① S_n → Traction normal to the shaded surface

$$\rightarrow S_n = T \cdot n = \begin{pmatrix} S_1 n_1 \\ S_2 n_2 \\ S_3 n_3 \end{pmatrix}(n_1\ n_2\ n_3) = S_1 n_1^2 + S_2 n_2^2 + S_3 n_3^2$$

projection of a vector

(shear stress)

② τ → Traction tangential to the shaded surface

By Pythagoras theorem, $\tau^2 = T^2 - S_n^2$

$$= [S_1^2 n_1^2 + S_2^2 n_2^2 + S_3^2 n_3^2] - [S_1 n_1^2 + S_2 n_2^2 + S_3 n_3^2]^2$$

$n_1^2 + n_2^2 + n_3^2 = 1$ ← unit normal vector

$$= (S_1 - S_2)^2 n_1^2 n_2^2 + (S_2 - S_3)^2 n_2^2 n_3^2 + (S_3 - S_1)^2 n_3^2 n_1^2$$

$$\therefore \tau = \sqrt{(S_1 - S_2)^2 n_1^2 n_2^2 + (S_2 - S_3)^2 n_2^2 n_3^2 + (S_3 - S_1)^2 n_3^2 n_1^2}$$

With a given fault plane with $\vec{n}$

$$\tau = \mu \cdot (S_n - P)$$

Fractured reservoirs and fluid flow
Critically stressed fault and conductive fault

- Examples
  - Majorities of hydraulically conductive faults are critically stressed

Hydraulically conductive **Hydraulically non-conductive**

Orientation of wells that would intersect the greatest number of critically stresses faults

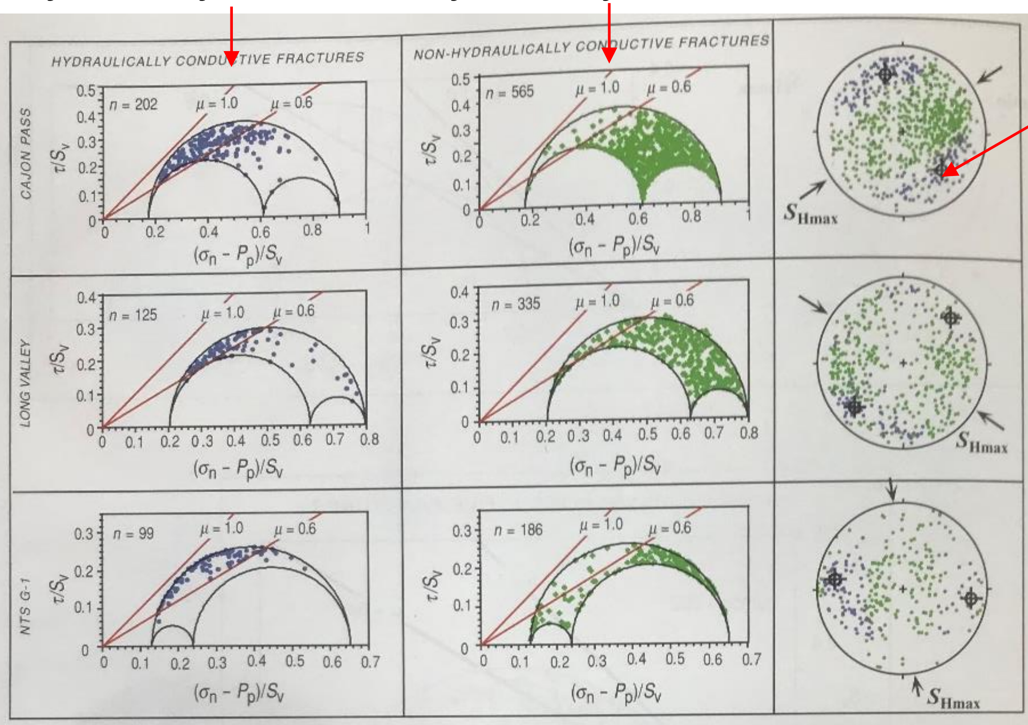

Figure 11.2. Normalized Mohr diagrams of the three wells that illustrate that most hydraulically conductive faults are critically stressed faults (left column) and faults that are not hydraulically conductive are not critically stressed (center column) along with stereonets that show the orientations of the respective fracture sets. The first row shows data from the Cajon Pass well (same Mohr diagrams as in Figure 11.1b), the second from the Long Valley Exploration Well and the third from well G-1 at the Nevada Test Site. After Barton, Zoback *et al.* (1995).

Cajon Pass
- Fractured Granite/granodiorate
- ~ 3.5 km
- ~ 4 km from the San Andreas fault
- Strike-slip ~ normal faulting

Long Valley:
- Fractured metamorphic rock
- drilled ~ 2 km
- Investigation of the structure/caldera
- Strike-slip ~normal-slip stress regime

Nevada Test Site (Yucca Mountain project)
- Tuffaceous rock
- potential site for nuclear waste repository
- Hole was drilled >1.7 km
- Normal faulting

Zoback MD, 2007, Reservoir Geomechanics, Cambridge University Press

Fractured reservoirs and fluid flow
Critically stressed fault and conductive fault

SEOUL NATIONAL UNIVERSITY

- Examples
  - Majorities of hydraulically conductive faults are critically stressed

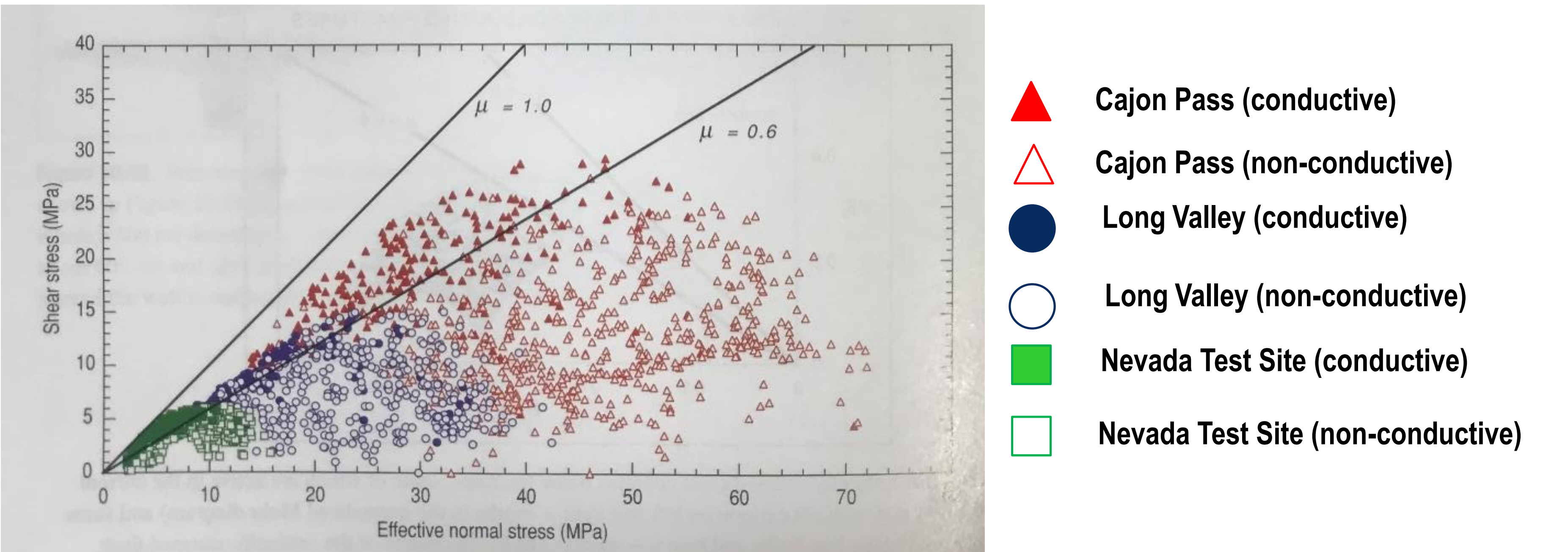

Figure 11.3. Shear and normal stresses on fractures identified with borehole imaging in Cajon P (triangles), Long Valley (circles), and Nevada Test Site (squares) boreholes. Filled symbols represent hydraulically conductive fractures and faults, and open symbols represent non-conductive fractures. From Townend and Zoback (2000) based on original data in Barton, Zoback *et al.* (1995).

Zoback MD, 2007, Reservoir Geomechanics, Cambridge University Press

Fractured reservoirs and fluid flow
Critically stressed fault and conductive fault

- Direction of fluid flow (permeability anisotropy)

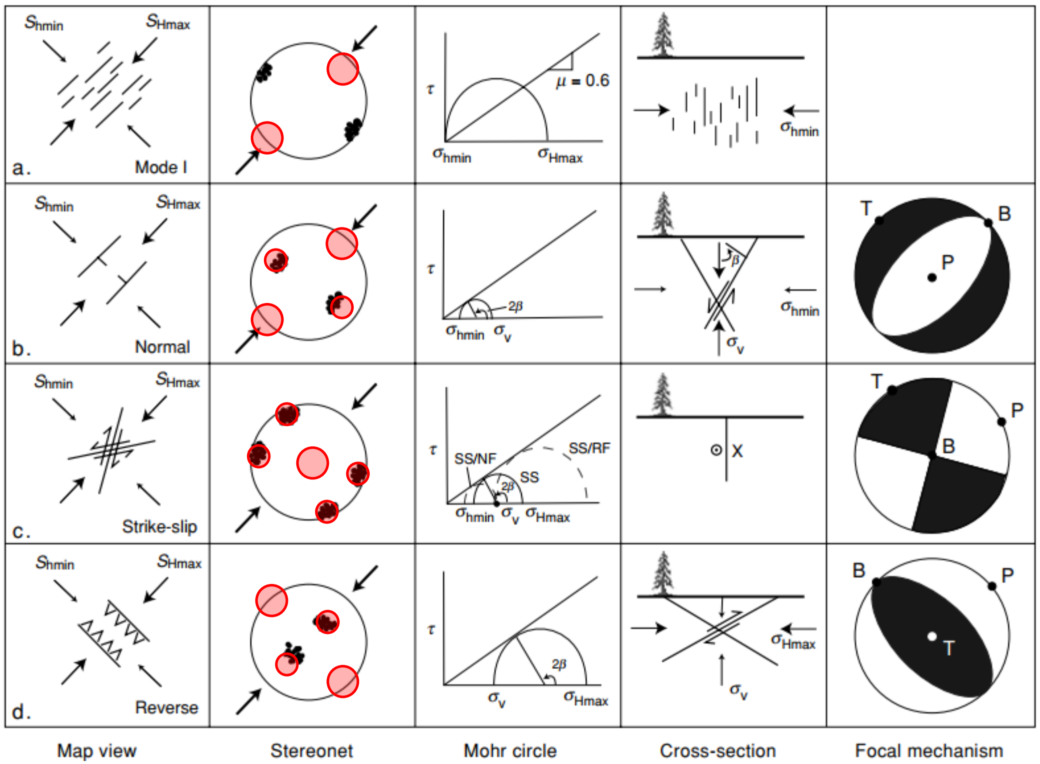

Direction of the largest permeability

Direction of the 2nd largest permeability

Zoback MD, 2007, Reservoir Geomechanics, Cambridge University Press

Fractured reservoirs and fluid flow
Critically stressed fault and conductive fault

SEOUL NATIONAL UNIVERSITY

- Relationship between critically stressed fault orientation and in situ stress

CFF: Shear stress minus resistance.
(-) no slip, (+) slip

Pp/Sv: relative pore pressure required for shear slip

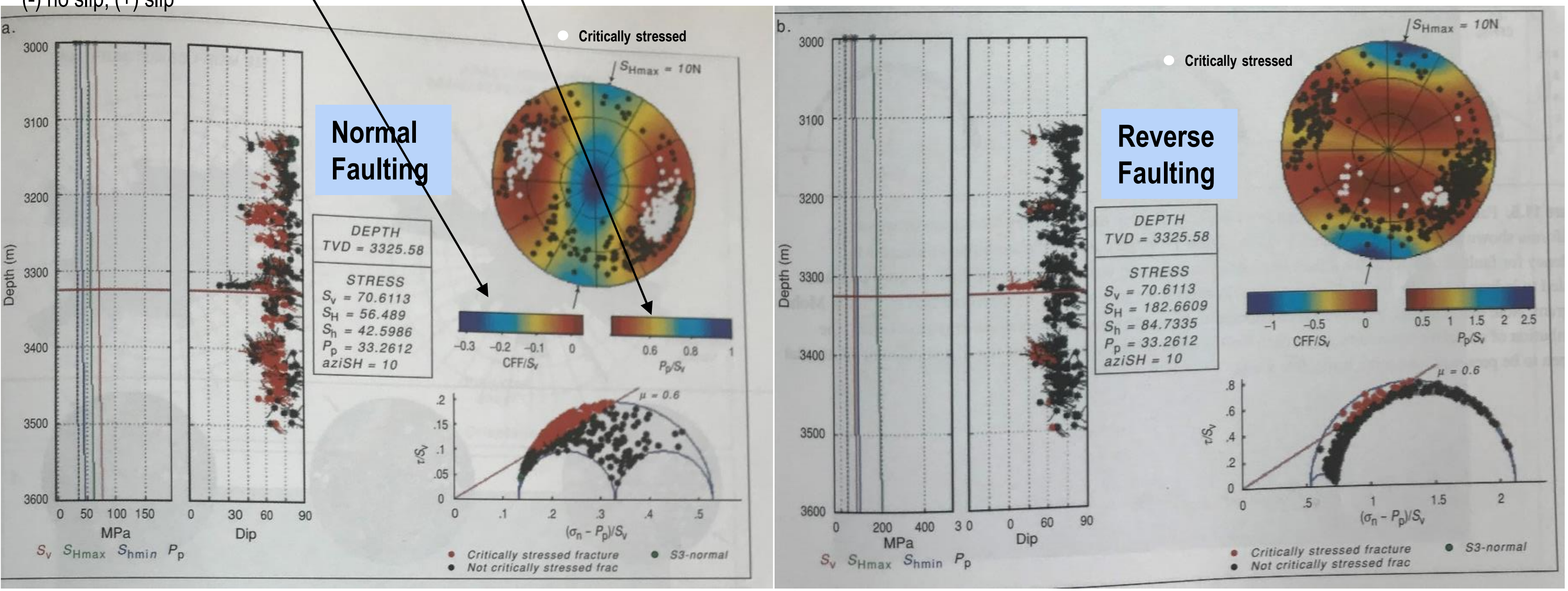

Zoback MD, 2007, Reservoir Geomechanics, Cambridge University Press

Fractured reservoirs and fluid flow
Critically stressed fault and conductive fault

SEOUL NATIONAL UNIVERSITY

- How to detect permeable faults or measure permeability

Table 11.1. *Detection of permeable faults and fractures in wells*

Technique	Basis	Depth of investigation	Benefits	Drawbacks
Packer tests	Isolation of specific faults and fractures using packers allows the transmissivity (permeability times thickness) to be measured directly	Fault permeability in region surrounding the wellbore.	Determines absolute permeability	Very time consuming and costly to test numerous intervals
Thermal anomalies	Measures flow-induced thermal anomalies	Near wellbore	Easy to acquire and process data	Difficult to use if temperature log is noisy or if there are so many closely spaced fractures and faults that it is difficult to interpret
Electrical images	Quantifies electrical conductivity of fractures with respect to host rock	Near wellbore	Easy to acquire image data and identify fractures	Assumes fluid flow and electrical properties are related at the wellbore wall
Stoneley-wave analysis	Permeable fractures attenuate Stoneley waves	Near wellbore	Straightforward to implement and carry out waveform analysis	Relatively insensitive. Stoneley wave attenuation can be caused by various factors
"Spinner" flowmeter logs	Measures variation of flow rate with depth as the logging tool is lowered, or raised, in the well	Formation surrounding the wellbore	Directly measures fluid flow	Requires high flow rates

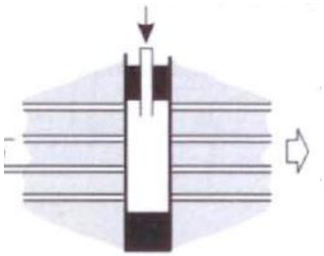

Zoback MD, 2007, Reservoir Geomechanics, Cambridge University Press

Fractured reservoirs and fluid flow
Detection of permeable fault - Temperature Logging

SEOUL NATIONAL UNIVERSITY

- Measure bore fluid not surrounding rock.
- It takes time to re-equilbrate with recently drilled hole
- The amount of time ~ magnitude of disturbance. ~ 10-20 times of drilling time required.
- Temperature anomaly
  - Can be used to detect natural fractures and hydraulic fractures

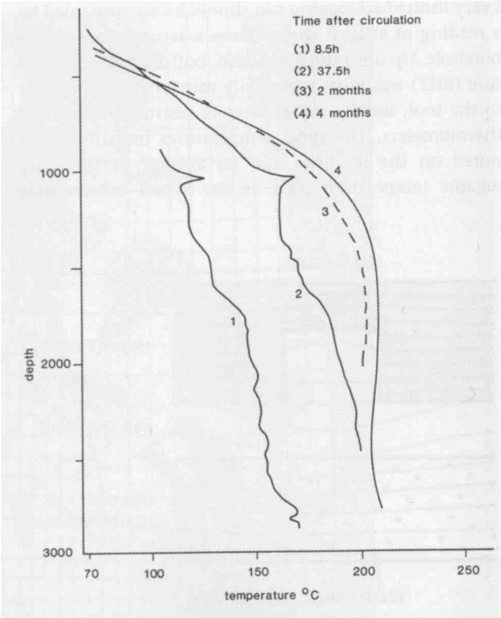

Change in borehole temperature with time

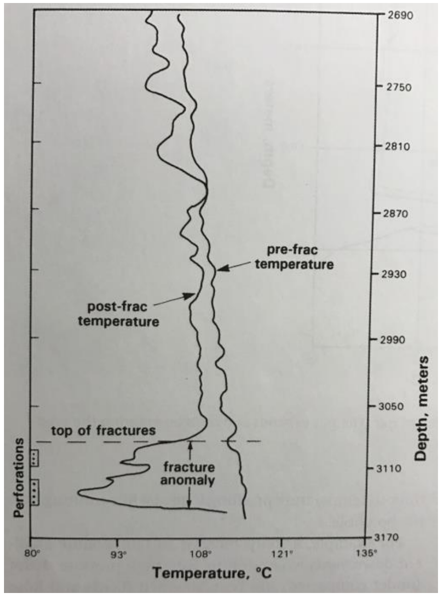

Temperature anomaly by hydraulic fracturing

Rider M and Kennedy M, 2011, The geological interpretation of well logs, 3rd ed., Rider French

Fractured reservoirs and fluid flow
Detection of permeable fault - Spinner log

SEOUL NATIONAL UNIVERSITY

- Spinner
  - An impeller used to measure fluid velocity
  - Frequency proportional to the relative velocity between the tool and fluid

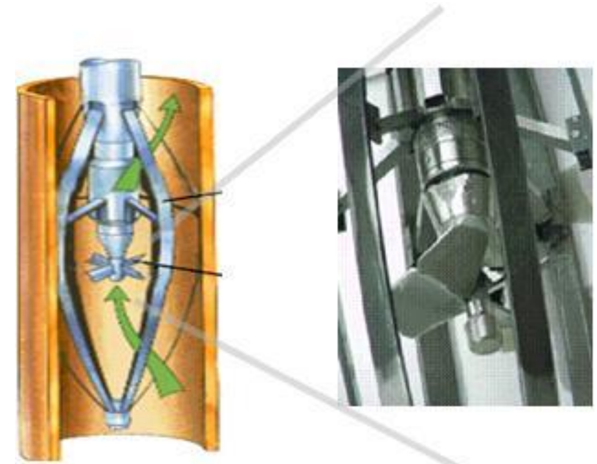

http://www.geothermal.uq.edu.au/06-October-2010

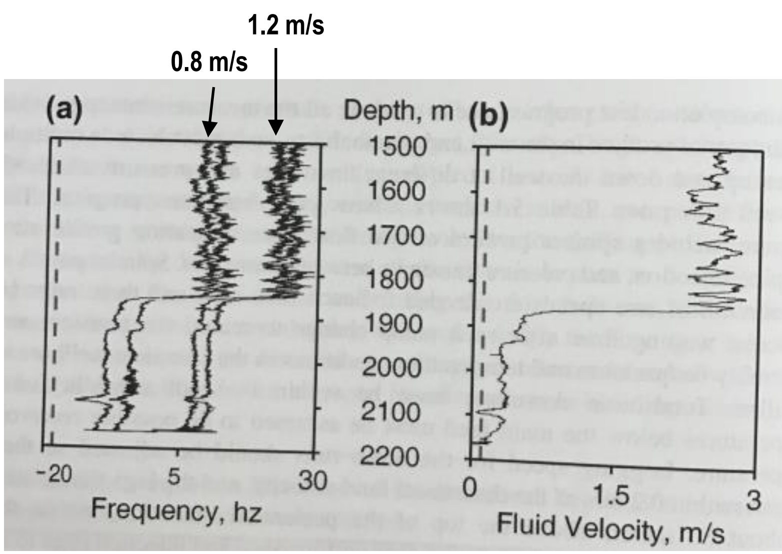

Permeable zone
(fractures in fractured reservoir)

Rider M and Kennedy M, 2011, The geological interpretation of well logs, 3rd ed., Rider French

Critically stressed faults
Case Studies

SEOUL NATIONAL UNIVERSITY

- Example (Monterey formation, California)
  - Under the same in situ stress condition, orientations of fractures are different and direction of major fluid flow varies

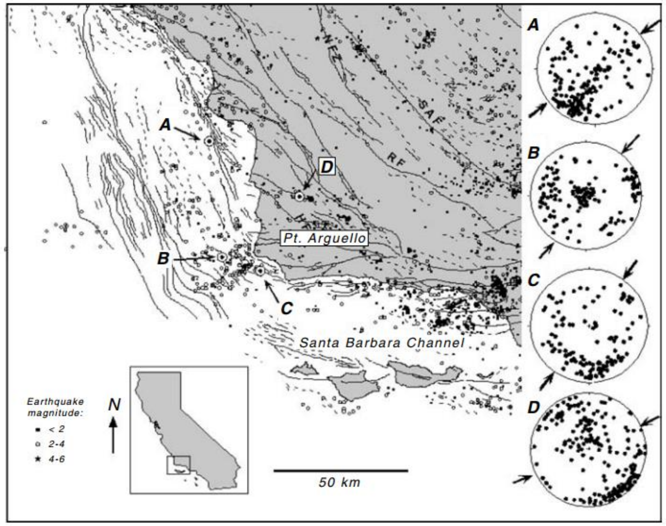

Critically stressed fault: Reverse fault

Critically stressed fault: Strike-slip

Critically stressed fault: Strike-slip

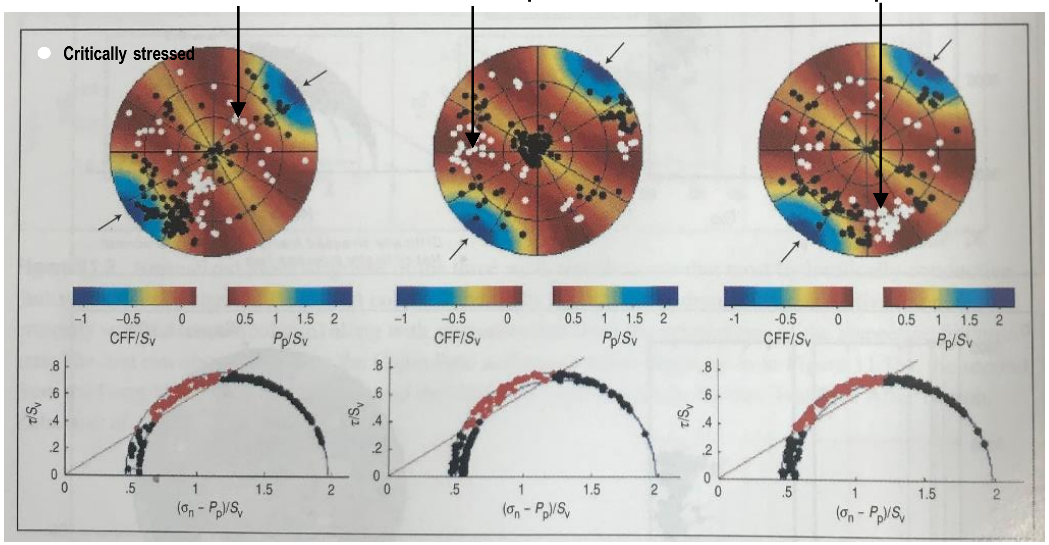

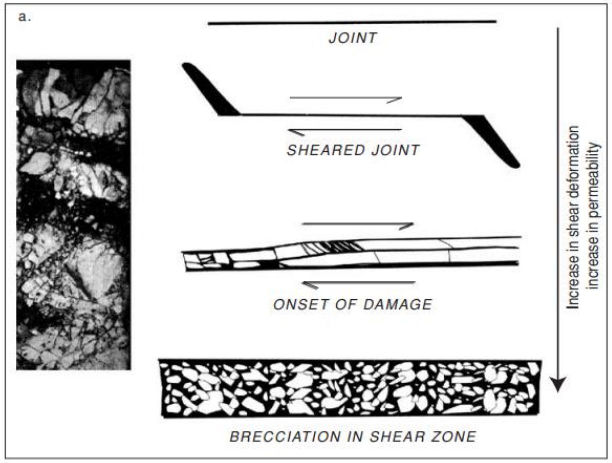

Zoback MD, 2007, Reservoir Geomechanics, Cambridge University Press

Critically stressed faults
Case Studies

SEOUL NATIONAL UNIVERSITY

- Example (Monterey formation, California)
  - Permeability may not increase even at critically stressed fault

Controlling factor of fault permeability increase

- **Degree of alteration and cementation of brecciated rock (fault sealing**
- **Diagenetic history**
- **Current effective normal stress**
- **Precipitation in the fault**

Diagenically immature shale (속성이 덜된 셰일) → slip may not contribute to permeability increase

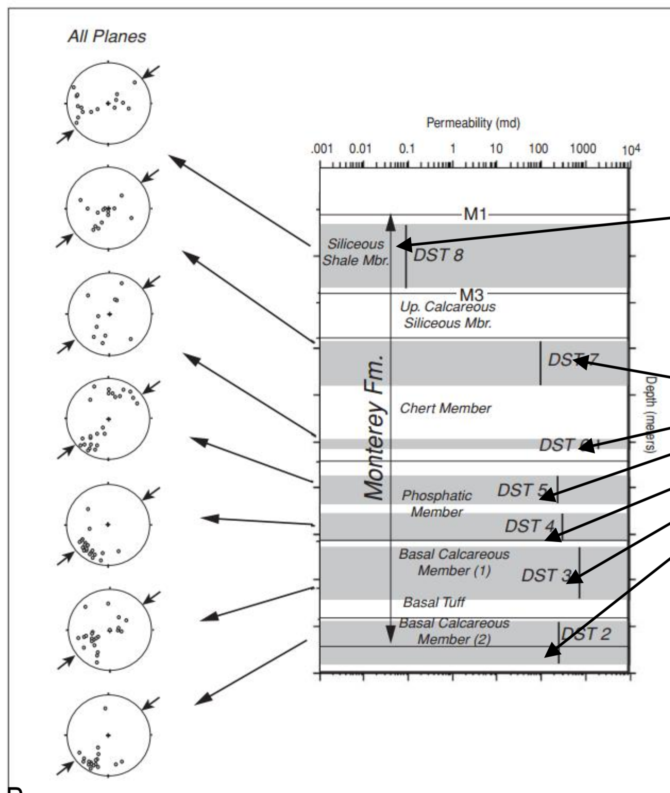

Permeability ~0.1 md

Permeability ~100~1,000 md

Zoback MD, 2007, Reservoir Geomechanics, Cambridge University Press

Critically stressed faults
Case Studies

- Example: Sellafield project, UK
  - Strike-slip faulting regime
  - The orientation of permeable faults is exactly by hypothesis of 'critically stress fault'.

All fractures **Fractures from transmissive zone only**

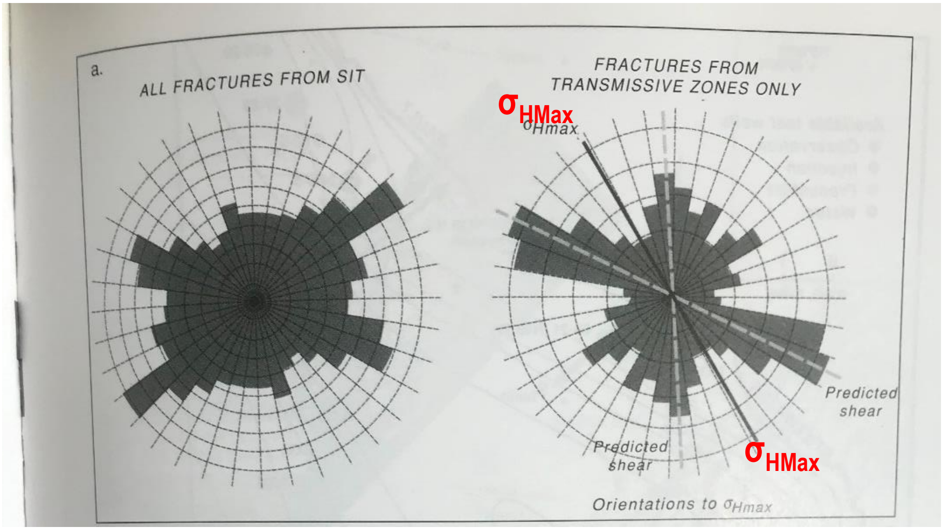

Zoback MD, 2007, Reservoir Geomechanics, Cambridge University Press

Critically stressed faults
Case Studies

- Example: Dixie Valley (Geothermal)
  - Competition:

competition

sealing due to precipitation in the fault ⟷ Creation of permeability due to dilation and brecciation

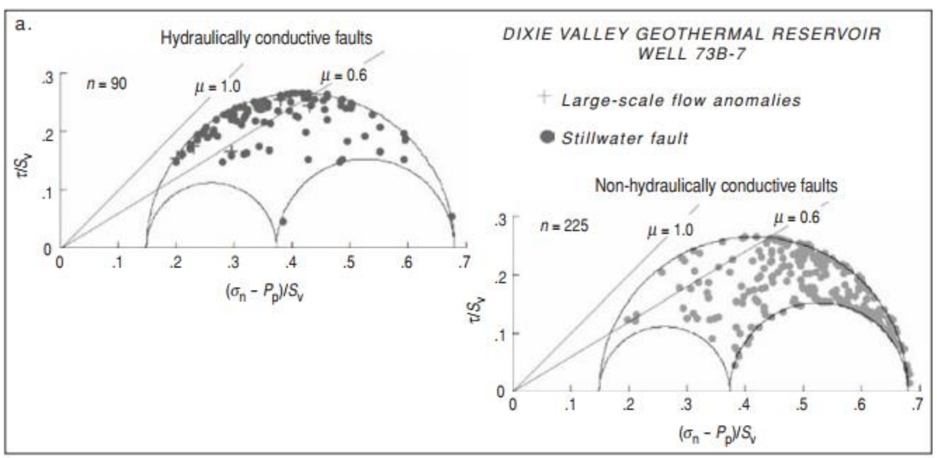

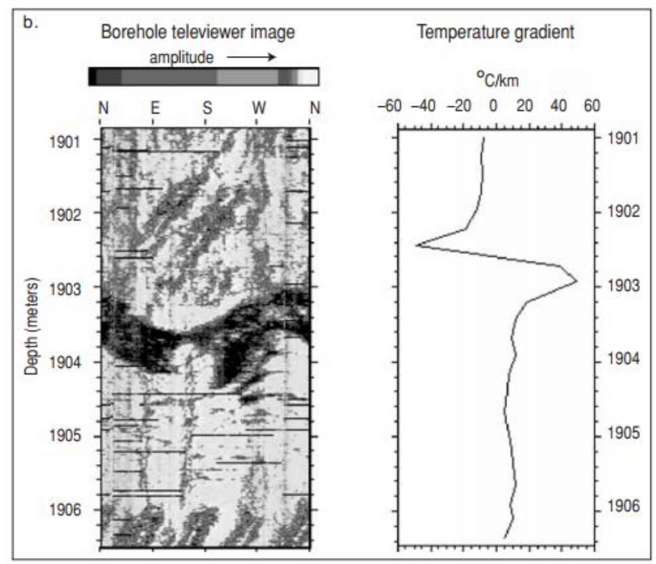

Zoback MD, 2007, Reservoir Geomechanics, Cambridge University Press

Identification of critically stressed faults and breakout rotations

SEOUL NATIONAL UNIVERSITY

- Fluctuations of stress orientation around the active faults due to fault slip

Results

Predicted vs. Measured stress (KLX04)

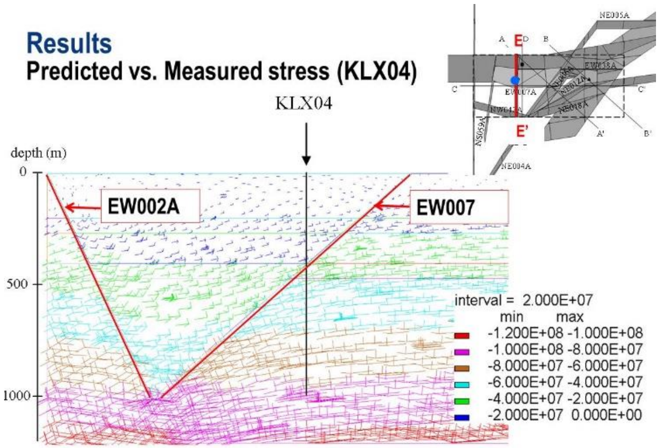

Borehole passes deformation zone EW007 at around 300 ~ 400 m depth
Dramatic change of stress occur due to the deformation zone – smaller stress in the wedge formed by two deformation zones (EW002A and EW007A).

Min (2008)

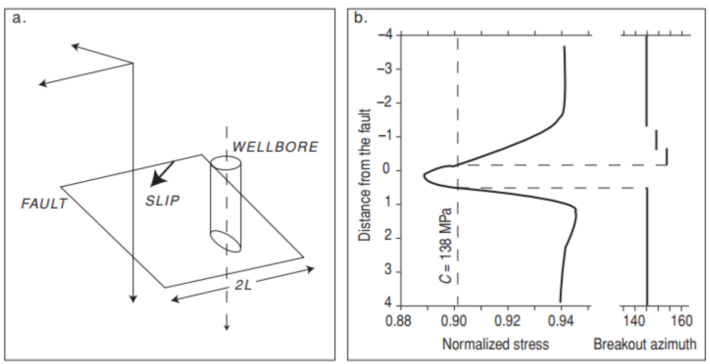

Breakout orientation fluctuations

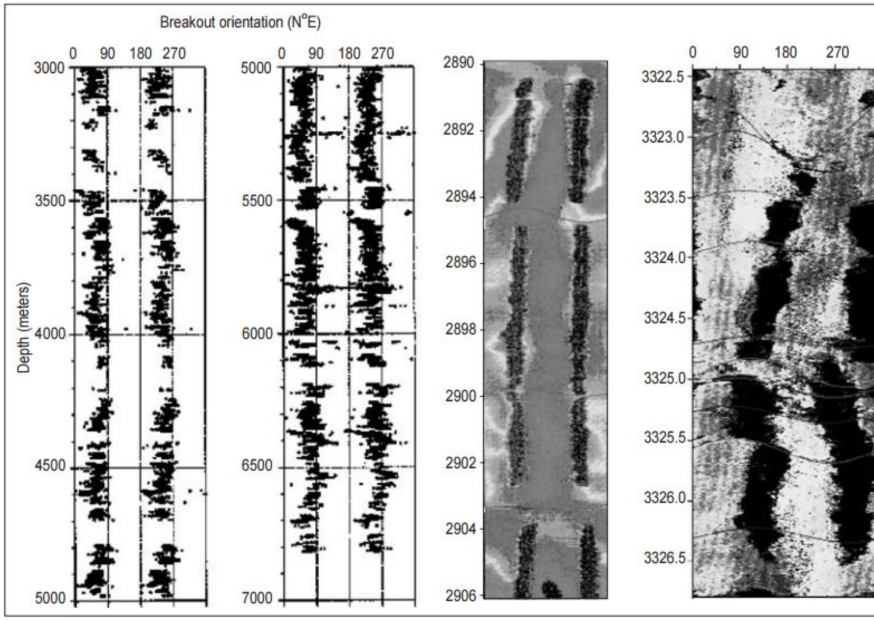

KTB borehole **Cajon Pass research hole**

Min KB, Effect of Deformation Zones on the State of *In Situ* Stress at a Candidate Site of Geological Repository of Nuclear Waste in Sweden, *Tunnel & Underground Space: Journal of Korean Society for Rock Mechanics*, 2008;18(2):134-148
Zoback MD, 2007, Reservoir Geomechanics, Cambridge University Press

Intentionally induced microseismicity to enhance permeability

SEOUL NATIONAL UNIVERSITY

- Critically stressed fault can be used for hydraulic stimulation
- Example at Yufutsu gas field (Japan)
  - Injection: 5,000m^3 for 7 days
  - Seismicity parallel to S_{HMAX}

Figure 11.12. Perspective view of four wells in the Yufutsu gas field, some of the larger faults in the reservoir and the cloud of microseismicity induced by injection of 5000 m^3 of water over 7 days (after Tezuka 2006). The cloud of seismicity is elongated along the direction of the vertical plane of a hydrofrac at the azimuth of S_{Hmax}.

Zoback MD, 2007, Reservoir Geomechanics, Cambridge University Press

Fault seal/blown trap

SEOUL NATIONAL UNIVERSITY

- Critically stressed faults cut through reservoir
  - Evidence of potentially large hydrocarbons in the past but not present today: *blown trap* problem

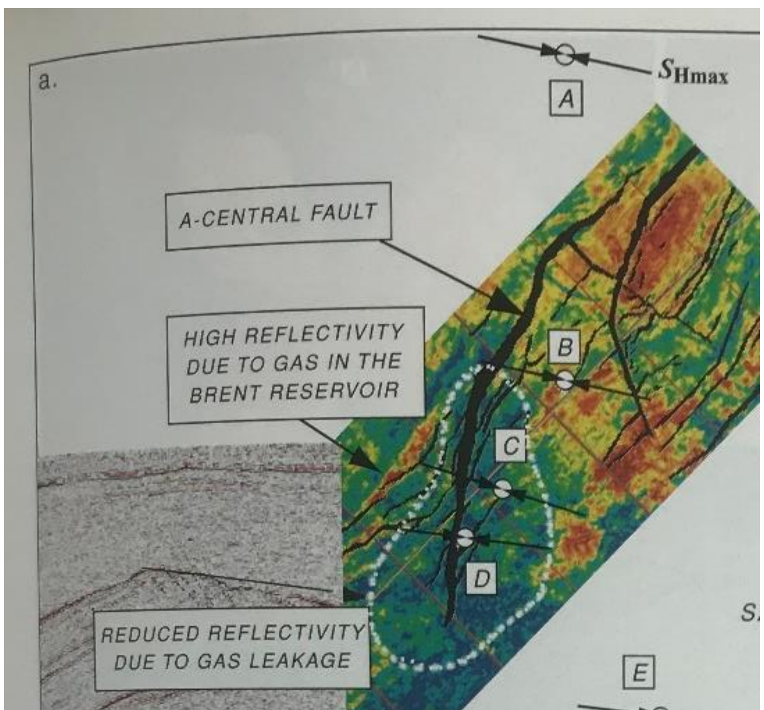

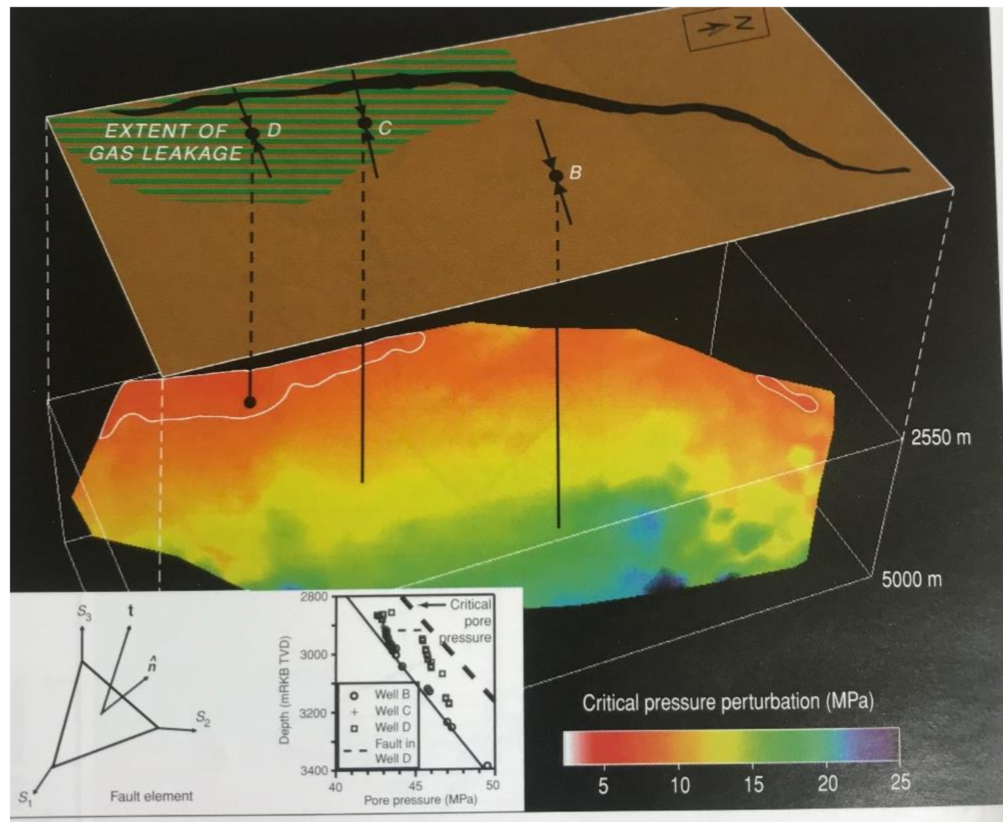

Zoback MD, 2007, Reservoir Geomechanics, Cambridge University Press

Dynamic constraints on hydrocarbon migration

SEOUL NATIONAL UNIVERSITY

- Geomechanical analysis such as shear slip potential can give insight into the hydrocarbon migration mechanisms

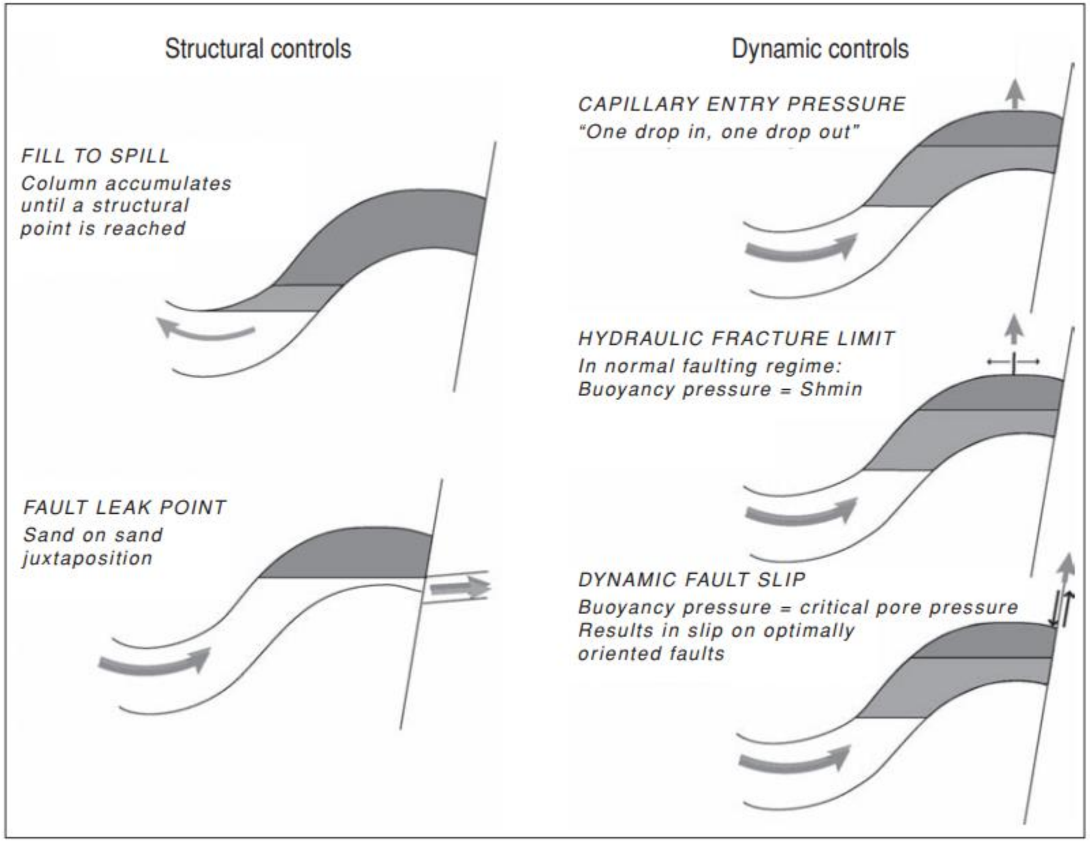

Zoback MD, 2007, Reservoir Geomechanics, Cambridge University Press